



**HAL**  
open science

## Bioaccumulation of Lithium Isotopes in Mussel Soft Tissues and Implications for Coastal Environments

Fanny Thibon, Marc Metian, François Oberhänsli, Maryline Montanes, Emilia Vassileva, Anna Maria Orani, Philippe Telouk, Peter Swarzenski, Nathalie Vigier

► **To cite this version:**

Fanny Thibon, Marc Metian, François Oberhänsli, Maryline Montanes, Emilia Vassileva, et al.. Bioaccumulation of Lithium Isotopes in Mussel Soft Tissues and Implications for Coastal Environments. ACS Earth and Space Chemistry, 2021, 5 (6), pp.1407-1417. 10.1021/acsearthspacechem.1c00045 . hal-03405883

**HAL Id: hal-03405883**

**<https://hal.science/hal-03405883>**

Submitted on 27 Oct 2021

**HAL** is a multi-disciplinary open access archive for the deposit and dissemination of scientific research documents, whether they are published or not. The documents may come from teaching and research institutions in France or abroad, or from public or private research centers.

L'archive ouverte pluridisciplinaire **HAL**, est destinée au dépôt et à la diffusion de documents scientifiques de niveau recherche, publiés ou non, émanant des établissements d'enseignement et de recherche français ou étrangers, des laboratoires publics ou privés.

1     **Bioaccumulation of lithium isotopes in mussel soft**  
2     **tissues and implications for coastal environments**

3     *Fanny Thibon<sup>a\*</sup>, Marc Metian<sup>b</sup>, François Oberhänsli<sup>b</sup>, Maryline Montanes<sup>a</sup>, Emilia Vassileva<sup>b</sup>,*  
4     *Anna Maria Orani<sup>b</sup>, Philippe Telouk<sup>c</sup>, Peter Swarzenski<sup>b</sup> and Nathalie Vigier<sup>a</sup>*

5

6     <sup>a</sup> Laboratoire d'Océanographie de Villefranche-sur-Mer (LOV), CNRS UMR 7093, Sorbonne  
7     université, 06230 Villefranche-sur-Mer, France

8     <sup>b</sup> International Atomic Energy Agency (IAEA), Environment Laboratories, 4a, Quai Antoine 1er,  
9     MC-98000 Principality of Monaco, Monaco

10    <sup>c</sup> Laboratoire de Géologie de Lyon, Ecole Normale Supérieure de Lyon, CNRS UMR 5276,  
11    Université de Lyon, 46 Allée d'Italie, 69007 Lyon, France

12

13 ABSTRACT

14 Lithium production has dramatically increased over the past decade, and first cases of  
15 environmental Li pollution have been recently reported in urban and in mining regions. While  
16 elevated Li concentrations may be toxic for living organisms, tools to monitor Li in the  
17 environment have not yet been developed. Consequently, its impact on key biota and human  
18 health is still poorly known. The present laboratory-based study shows that the soft tissue of blue  
19 mussels (*Mytilus edulis*) can be used to quantify Li contamination in coastal waters. Stable Li  
20 isotope ratios ( $^7\text{Li}/^6\text{Li}$ ) measured in these soft tissues correlate positively with seawater Li  
21 concentrations and show precisely the threshold above which mussels shift their depuration  
22 mechanism. Combined with other data from the natural environment, the experimental results  
23 have profound implications for the fate of coastal ecosystems and shellfish consumption living  
24 under high Li environmental level. We also highlight the need to develop innovative tools to  
25 extract Li from wastewaters before its release into rivers and, ultimately, the ocean.

26 KEYWORDS

27 Bivalves, Lithium, Isotopic tools, Emerging contaminant, Fractionation, Concentration effects

28

29 **Introduction**

30

31 Lithium (Li) occurs naturally at trace levels in the environment. Consequently, it is also present  
32 in living organisms, and some studies have even suggested that Li should be recognized as an  
33 essential element<sup>1</sup>. However, as observed for other metals<sup>2,3</sup>, Li is toxic and can eventually be  
34 lethal beyond a specific threshold<sup>4-6</sup>. Elevated levels of Li in the aquatic environment can be due  
35 to natural inputs, mainly from rock erosion<sup>7</sup>, but they can also be related to anthropogenic  
36 activities. There is an increasing demand of Li from high-tech industries producing Li-rich  
37 batteries for laptops, mobiles, and other electronic devices worldwide. The Li production has  
38 increased from 23 to 33 kt.yr<sup>-1</sup> during 2010–2017<sup>8-10</sup>, and the demand for Li is expected to  
39 follow the greatest growth trajectory among all metals by 2025<sup>9</sup>. Li contamination has already  
40 been observed in groundwater and river water with close proximity to mining sites<sup>11</sup>, as well as  
41 in municipal waters of a modern and densely populated metropolitan area<sup>12</sup>. This is a worrying  
42 problem as the various protocols of wastewater depuration appear to be inefficient<sup>12</sup> at removing  
43 Li because of the high mobility of Li and its poor ability to adsorb onto particle surfaces<sup>13</sup> (Li  
44 was used as an aquifer water flux tracer<sup>14,15</sup>). In addition, there is no major Li sink in estuaries  
45 and, therefore, dissolved Li is conservatively delivered to littoral waters and to the ocean<sup>16,17</sup>.  
46 Overall, there is a growing concern on the fate of global Li increase in the environment,  
47 especially the risk of this emerging aquatic pollution on organisms and humans that consume  
48 them.

49 Li monitoring in the marine environment is not commonly performed as compared to other trace  
50 metals<sup>18-20</sup>. For instance, mussel-based biomonitoring programs<sup>21-23</sup> do not include Li in the

51 chemicals analyzed, even if mussels, along with other shellfish and bivalves, contain more Li  
52 than any other species from higher trophic levels<sup>24</sup>. The paucity of information on the process of  
53 Li accumulation in marine coastal organisms needs to be addressed to better understand the  
54 response, the fate, and the risk of Li contamination in the marine environment, as well as for  
55 potential human health implications.

56 To better comprehend the biological mechanisms at play, it is possible to measure precisely the  
57 natural variations of Li stable isotope ratios (<sup>6</sup>Li and <sup>7</sup>Li, abundances of 7.59% and 92.41%,  
58 respectively). Stable isotopes of trace metals are valuable tools to investigate subtle  
59 physiological changes in organisms<sup>25–28</sup>. However, Li isotopes in marine organisms were, so far,  
60 not used due to technical limitations related to low Li levels in tissues<sup>29</sup>. Yet, being able to  
61 measure and track Li isotopes in this manner (1) will help understand how they are affected by  
62 homeostatic processes and elevated Li levels in the environment, and (2) will also benefit paleo-  
63 oceanographic studies wherein Li has proven utility. Indeed, Li isotopes are now widely used to  
64 reconstruct past ocean and climate by analyzing fossil carbonates formed by calcifying  
65 organisms<sup>30–34</sup>. However, the role and impact of biological processes (‘vital effects’) on these  
66 biogenic minerals still remain an open question<sup>35–38</sup>, which leads to a high level of uncertainties  
67 concerning Earth’s climate regulation after a disturbance, such as from a meteorite impact or a  
68 mass extinction<sup>39</sup>.

69 Here, we exposed blue mussels (*Mytilus edulis*) to various degrees of environmental Li  
70 enrichment during laboratory experiments. We report Li concentrations and Li isotopes  
71 compositions of mussel soft tissues. We aim to define the impact of elevated Li levels in mussel  
72 metabolism and, by comparing our results with data collected in the natural environment, to  
73 evaluate the mussel ability to biomonitor Li contamination. We also highlight the Li

74 environmental concentration limit that defines risk for bivalves and assess implications of  
75 elevated Li concentrations for coastal organisms and population.

76

## 77 **Materials and Methods**

78

### 79 ***Experimental setting and sample preparation***

80 A summary of the experimental setting is sketched in Fig. S1. Forty individual common blue  
81 mussels (*Mytilus edulis*) of similar size ( $43.01 \pm 2.18$  mm) and wet weight ( $7.137 \pm 1.014$  g)  
82 were collected in summer 2019 (outside spawning period) *in situ* from La Rochelle, Bay of  
83 Biscay, France. The experiment was performed at the Environment Laboratories of the  
84 International Atomic Energy Agency (Monaco), based on well-established protocols. Mussels  
85 were acclimated at the laboratory environment for one month, at  $20.5^{\circ}\text{C}$ . Batches of five mussels  
86 were placed in eight 5-L glass beakers filled with 2 L of filtered (1  $\mu\text{m}$ ) seawater pumped from  
87 the 30m water depth in Mediterranean Sea (Monaco Bay). Seawater salinity, temperature, and  
88  $\text{pH}_T$  were  $39 \pm 1$ ,  $20.5 \pm 0.5$   $^{\circ}\text{C}$ , and  $8.03 \pm 0.05$ , respectively. Water oxygenation was ensured  
89 by constant air bubbling, and a 12 h-12 h light-dark cycle was established.

90 Two duplicates (A and B) of four experimental conditions were implemented with increasing  
91 seawater Li concentrations: CTRL (control group,  $\sim 0.18$  mg Li  $\text{L}^{-1}$ ), Li-0.5 ( $\sim 0.5$  mg Li  $\text{L}^{-1}$ ), Li-  
92 1.0 ( $\sim 1.0$  mg Li  $\text{L}^{-1}$ ), and Li-1.5 ( $\sim 1.5$  mg Li  $\text{L}^{-1}$ ). To obtain the desired Li concentrations,  
93 dedicated volumes of a concentrated Li reference solution (1000 mg Li  $\text{L}^{-1}$ , ICP Standard) were  
94 evaporated and added as solid salt to the filtered seawater.

95 The mussels were kept in their experimental aquaria during 4 days, and the culture media  
96 (seawater with different Li concentrations) were renewed every day at the same time ( $13:40 \pm 40$

97 min). Due to the paucity of data on Li bioaccumulation process, we decided (1) to investigate the  
98 short time process in order to better understand the short term isotope fractionation and uptake  
99 processes assuming that Li should act like other alkali elements (i.e., Cs, which quickly reaches a  
100 saturation state when accumulated in marine bivalves<sup>40-42</sup>) and (2) to use a relatively high  
101 exposure concentration based on data available in freshwater studies<sup>4,43</sup>. Seawater samples were  
102 collected before and after each water change to confirm that each aquarium operated as an open  
103 system. Between water changes, the mussels were fed for 1 h using non-contaminated seawater  
104 containing phytoplankton *Isochrysis galbana* at a concentration of  $10^4$  cells mL<sup>-1</sup>. One mussel  
105 died after 2 days of the experiment in the duplicate A of the CTRL condition. At the end of the  
106 experiment, all individuals were collected and rinsed for 30 min in clean, filtered seawater  
107 following the classical protocol for eliminating weakly adsorbed elements from tissue samples<sup>44</sup>.  
108 The soft tissues were then extracted, frozen at -28 °C for 72 h, and freeze-dried for further  
109 analyses.

110

### 111 ***Analytical methods***

112 To minimize the possibility of any contamination and procedural blanks, all analytical  
113 preparations were performed in a positively pressurized clean laboratory under a fume-hood  
114 using only distilled, trace-metal grade reagents and pre-cleaned vessels. Each mussel's soft tissue  
115 was weighed in a Teflon reactor, then digested in a mixture of 5 mL HNO<sub>3</sub> and 2 mL H<sub>2</sub>O<sub>2</sub> (both  
116 trace metal grade, Fisher Scientific, USA) at 90 °C for ~5 h. The obtained solutions were  
117 transferred into pre-cleaned polyethylene tubes and gravimetrically diluted up to 20 g with  
118 MilliQ water (18 MΩ). Two procedural blanks and two replicates of the Certified Reference  
119 Material (CRM) IAEA 407 (Fish Homogenate, IAEA, Vienna) were included in the digestion

120 batch and analyzed with the samples. The recoveries obtained for the CRM were 95±3 %. For  
121 each sample, two solution aliquots were separated for elemental and isotopic analyses.

122 Lithium concentrations were determined at the IAEA in Monaco by flame atomic absorption  
123 spectroscopy using a ContrAA 700 (Analytic Jena, Germany). The applied analytical procedure  
124 was based on external calibration approach and was preliminary validated, according to the  
125 requirements of international guidelines for method validation<sup>45</sup>. Calibration curves were daily  
126 prepared using proper dilution of commercially available standard solutions. All possible sources  
127 of uncertainty of obtained results were carefully identified. The numerical method of  
128 differentiation described by Kragten<sup>46</sup> was used to calculate combined standard uncertainties of  
129 obtained measurement results.

130 Prior to Li isotopic analyses, the Li in the samples must be purified. Lithium extraction and  
131 purification were performed following the procedure of Vigier *et al.*<sup>47</sup>, summarized here.  
132 Sample solution aliquots were dried out and taken up in 0.5 mL of 1 N HCl and loaded on AG  
133 50-X12 cationic resin in 8.5-cm-high Teflon columns. Lithium was purified twice with 1 N HCl.  
134 This fraction was evaporated to dryness before the analysis.

135 Lithium has two naturally occurring isotopes, one heavy (<sup>7</sup>Li, 92.41% abundance) and one light  
136 (<sup>6</sup>Li, 7.59% abundance). The isotopic compositions of geological and biological materials are  
137 reported as per-mil variations relative to an isotopic standard (here LSVEC) as  $\delta^7\text{Li}_{\text{sample}} [\text{‰}] =$   
138  $((^7\text{Li}/^6\text{Li})_{\text{sample}} / (^7\text{Li}/^6\text{Li})_{\text{LSVEC}} - 1) \times 1,000$ .

139 Lithium isotopic analyses were performed at the CNRS-INSU National Service based at the  
140 École Normale Supérieure de Lyon (France) using a Thermo-Fisher Neptune *Plus* multi-  
141 collector inductively coupled plasma mass spectrometer following the procedure of Balter and  
142 Vigier<sup>29</sup> and Bastian *et al.*<sup>48</sup> developed for low Li concentrations in biological materials. In brief,



143 samples and standards were analyzed under dry plasma conditions in low-resolution mode.  
144 Instrumental mass bias correction was performed externally using the standard bracketing  
145 method (using the LSVEC reference material). Analytical blanks, as well as total procedural  
146 blanks, were found to be negligible. The internal reproducibility was on average  $\pm 0.04\%$ .  
147 Precision (external reproducibility), estimated from two to three replicate measurements of 14  
148 different samples (mussels and water), ranged from 0.04 to 1.91‰ with an average of  $\pm 0.5\%$ . In  
149 general, the accuracy of reported isotopic compositions are estimated based on analyses of  
150 reference materials of known isotopic composition. However, the Li isotopic compositions of  
151 biological reference materials corresponding to soft tissue have never been characterized. Thus,  
152 this study reports for the first time the Li isotopic composition of a soft-tissue biological  
153 reference material IAEA 407 ( $\delta^7\text{Li} = 28.3 \pm 1.7\%$ , 2SD,  $n = 2$ ). For comparison, the  
154 reproducibility of  $\delta^7\text{Li}$  obtained for the Li7-N non-biological reference material was 0.4‰ (2SD,  
155  $n = 22$ )<sup>48</sup>. Note that the IAEA 407 contain  $0.68 \pm 0.1 \mu\text{g Li g}^{-1}$  of dry powder, while Li7-N is an  
156 isotopically homogeneous solution, analyzed at a Li concentration of  $4 \text{ ng mL}^{-1}$ .

157

### 158 ***Statistical treatment***

159 Since the Li data were not normally distributed (i.e., Li concentration and Li isotope ratios do not  
160 follow a normal law), we adopted non-parametric statistical tests. The Mann-Whitney-Wilcoxon  
161 test was used to compare median values between two observational series, and the Kruskal-  
162 Wallis test was used to compare three or more series. Tests were performed using R software<sup>49</sup>  
163 using the respective functions *wilcox.test* and *kruskal.test*. The level of significance for statistical  
164 analyses was set at  $p < 0.05$ .

165 The relationship between quantitative variables was investigated using principal component  
166 analysis (PCA, see section 4.3), a statistical tool that reduces the number of original quantitative  
167 variables to fewer dimensions that may explain the majority of the observed variability. Here,  
168 PCA was performed using R software <sup>49</sup> considering the following variables: Al, B, Ca, Fe, K,  
169 Li, Mg, Mn, Na, Si, and Sr concentrations in mussels, the Li concentration in seawater ( $Li_{sw}$ ),  
170 and  $\Delta^7Li_{mussel-water}$ .

171

## 172 **Results**

173

174 In the control group ‘CTRL’, the aquarium seawater Li concentration was  $0.18 \mu g mL^{-1}$ , which  
175 corresponds to the mean global ocean Li concentration<sup>50</sup>. Li concentrations in seawater were set  
176 at 0.5, 1.0, and  $1.5 \mu g mL^{-1}$  in the ‘Li-0.5’, ‘Li-1.0’, and ‘Li-1.5’ treatments, respectively. The Li  
177 water concentration error is estimated at 10% (2SD). After the experiment, Li concentrations  
178 measured in mussels soft tissues were  $0.45 \pm 0.18$  for the CTRL group (2SD,  $n = 9$ ),  $1.20 \pm 0.53$   
179 (2SD,  $n = 10$ ),  $1.54 \pm 0.96$  (2SD,  $n = 10$ ), and  $2.19 \pm 1.65 \mu g g^{-1}$  (2SD,  $n = 10$ ), for the ‘Li-0.5’,  
180 ‘Li-1.0’, and ‘Li-1.5’ treatments, respectively (Fig. 1A, Table S2). This corresponds to a fivefold  
181 increase of the average mussel Li concentration between CTRL and Li-1.5, in response to an  
182 eightfold increase of the seawater Li concentration.

183 Due to the different isotopic compositions in seawater ( $\delta^7Li = 31.2 \pm 0.3\text{‰}$  in the open  
184 ocean<sup>50,51</sup>) and the pure Li solution ( $\delta^7Li = 10.8\text{‰}$ ) used to prepare the three exposure conditions,  
185 the mussels in each group were exposed to seawater with different Li isotopic compositions  
186 ( $\delta^7Li_{sw}$ , which remained constant over the course of the experiment; Table S1):  $\delta^7Li_{sw}^{CTRL} = 31.5$   
187  $\pm 0.7\text{‰}$  (2SD,  $n = 5$ ),  $\delta^7Li_{sw}^{Li-0.5} = 18\text{‰}$  (calculated),  $\delta^7Li_{sw}^{Li-1.0} = 14.6 \pm 0.01\text{‰}$  (2SD,  $n = 2$ ),

188 and  $\delta^7\text{Li}_{\text{sw}}^{\text{Li-1.5}} = 13.4 \pm 0.1\text{‰}$  (2SD,  $n = 5$ ). These compositions fit along a binary mixing curve  
189 (cf. following sections), which demonstrates that, despite a significant Li incorporation by  
190 mussels, it remains negligible when compared to the total water Li content of each aquarium. As  
191 a consequence, it does not modify neither the water Li content, nor its  $\delta^7\text{Li}$  value.  
192 The average  $\delta^7\text{Li}$  of mussel soft tissues in groups Li-1.0 and Li-1.5 were  $21.0 \pm 2.6\text{‰}$  and  $21.6 \pm$   
193  $2.7\text{‰}$ , respectively (Table S2, Fig. 1B). The one in group Li-0.5, significantly higher than the  
194 latest ( $24.4 \pm 3.4\text{‰}$ , Wilcoxon test,  $p < 0.001$ ) was significantly lower than that in the control  
195 group ( $31.7 \pm 2.0\text{‰}$ , Wilcoxon test,  $p < 0.0001$ ).

196

## 197 **Discussion**

198

### 199 ***Li bioaccumulation by mussels***

200 At the end of the experiment, the Li concentrations measured in mussels of the control group  
201 ( $0.45 \pm 0.18 \mu\text{g g}^{-1}$ ) were consistent with that observed in bivalve tissues and organs collected  
202 along the French Atlantic coast ( $0.43 \pm 0.25 \mu\text{g g}^{-1}$ )<sup>52</sup>. This result supports the representative  
203 nature of our samples, the reliability of our methods, as well as the lack of bias related to the  
204 experimental setup. In both cases (in experiments and in nature), mussel Li concentrations are  
205 significantly higher than in seawater ( $0.18 \mu\text{g mL}^{-1}$ ), by a factor of 2.5 on average. This agrees  
206 well with a recent study<sup>24</sup> that shows that bivalves, and filter feeders in general, accumulate Li  
207 the most compared to other organisms from higher trophic groups, such as crustaceans,  
208 cephalopods, and fish.

209 The average Li concentrations displayed by mussels exposed to Li-rich seawater are statistically  
210 higher than those of the control group, and increase with seawater Li concentrations, up  $2.19 \pm$

211 1.65  $\mu\text{g g}^{-1}$  when the water Li content is 1.5  $\mu\text{g mL}^{-1}$  (Figs. 1A and 2A). This demonstrates that,  
212 on average, mussels accumulate Li proportionally to the concentrations found in their  
213 environment, which is a major criterion to validate a biota as a reliable bioindicator of  
214 contamination<sup>53</sup>. These results are consistent with a recent laboratory study that explored key  
215 biochemical parameters changed by long-term (28 days) Li exposure on mussels. At 0.25 and  
216 0.75  $\text{mg Li L}^{-1}$  in aquarium water, the mussel Li concentrations were found to be  $0.9 \pm 0.23 \mu\text{g}$   
217  $\text{g}^{-1}$  and  $1.4 \pm 0.23 \mu\text{g g}^{-1}$ , respectively. These data perfectly fit with our short-term exposure  
218 results (Figure 2A), supporting that a bioaccumulation steady-state was reached within the 4-day  
219 exposure. The ability of bivalves to bioaccumulate Li can also be evidenced along the coast of  
220 North Chile (Table 1). Indeed, this coastal area is characterized by an unusually elevated Li  
221 concentration from river waters draining the high altitude Salars (salt flats). When compared to  
222 bivalves collected in low Li environments, such as the Atlantic or the Pacific coast, the Chilean  
223 bivalves display much higher Li concentrations (by 50 to 270 times higher, see Table 1). Taken  
224 altogether (Fig. 2A), all these data are consistent and demonstrate that mussels take up Li in  
225 direct proportion to the ambient dissolved concentrations, at least over the range of  
226 concentrations tested here.

227 There is a significant variability among individuals, and a striking observation is that this  
228 variability of individual Li concentrations increases with seawater Li concentration (from 44% in  
229 the control group to 75% in Li-1.5; Fig. 1A). This suggests that some mussels, when exposed to  
230 elevated Li concentrations, can better regulate Li uptake than others. This kind of intra-  
231 variability among mussels has already been reported for other trace elements such as Zn, Cd, and  
232 Cu<sup>18</sup>. Thus, a reliable assessment of environmental Li concentrations requires that several  
233 mussels are pooled together to capture the range of individual responses, as this is done for other

234 contaminants measured in bivalves<sup>21-23</sup>. Based on the range of seawater Li concentration used in  
235 this study, we estimate that accurate Li concentration can be obtained with the analyses of at  
236 least five individuals, and likely more when water Li concentration exceeds 1.5  $\mu\text{g mL}^{-1}$ , such as  
237 in Northern Chili (since the variability increases with the Li level, Fig. 2). Existing  
238 biomonitoring programs usually collect and pool between 80 and 160 individuals per site<sup>54</sup>, so  
239 the use of mussels to monitor Li levels along with other contaminants in coastal areas appear  
240 largely feasible.

241

### 242 *Preferential <sup>7</sup>Li enrichment in mussels*

243 While the seawater in experimental aquaria have a constant and homogenous  $\delta^7\text{Li}$  value for each  
244 condition, exposed mussels are ‘isotopically fractionated’ compared to their aquarium water, i.e.  
245 with significantly higher  $\delta^7\text{Li}$  values (Fig. 2B). This indicates that mussels preferentially  
246 accumulate the heavy (<sup>7</sup>Li) isotope in their soft-parts, as compared to the light (<sup>6</sup>Li) isotope. It is  
247 possible to calculate the corresponding water-mussel Li isotopic fractionations ( $\Delta^7\text{Li}_{\text{mussel-water}}$ )  
248 using<sup>55</sup>:

$$249 \quad \Delta^7\text{Li}_{\text{mussel-water}} (\text{‰}) = \delta^7\text{Li}_{\text{mussel}} - \delta^7\text{Li}_{\text{water}} \quad (1)$$

250  $\Delta^7\text{Li}_{\text{mussel-water}}$  value near 0‰ indicates no Li isotopic fractionation, since mussel  $\delta^7\text{Li}$  is equal to  
251 water  $\delta^7\text{Li}$ .

252 At the end of the exposition, the average  $\Delta^7\text{Li}_{\text{mussel-water}}$  ranges from 0.0‰ to +10.3‰ (Fig. 2B).  
253 Mussels in the control group exhibit a mean  $\delta^7\text{Li}$  value similar to that of the seawater (with  
254  $\Delta^7\text{Li}_{\text{mussel-water}} = +0.4 \pm 0.9\%$ , SD,  $n = 8$ ), whereas the average  $\Delta^7\text{Li}_{\text{mussel-water}}$  values of the other  
255 experimental groups increase from  $+5.7 \pm 2.1\%$  to  $+7.5 \pm 3.2\%$  (from Li-0.5 to Li-1.5  
256 respectively). Li isotopic fractionation is the strongest with the very first - limited - increment in

257 Li enrichment (5.7‰ in Li-0.5 condition vs. 0.4‰ in CTRL group). Further increases in seawater  
258 Li concentration still result in significant (Wilcoxon test,  $p < 0.05$ ), but lower, isotope  
259 fractionation (up to 7.5‰ in Li-1.5). This indicates that mussel  $\delta^7\text{Li}$  value increases with Li  
260 contamination and suggests that even an exposition to a small degree of contamination has a  
261 strong and significant effect on mussel Li isotopic compositions. The Li isotopic compositions of  
262 mussel soft tissues can therefore reveal even very subtle effects related to environmental Li  
263 contamination, which further supports the possibility to use mussel Li isotope ratio to monitor  
264 the Li level in waters. Measuring the isotopic composition of mussels has the advantage that  
265 there is small Li isotopic variability among mussel individuals and a representative  $\delta^7\text{Li}$  value  
266 requires 2 individuals only (for a 2–3‰ uncertainty), in contrast to Li concentration. Variabilities  
267 exists for isotopic composition, but their magnitude is only of few permill maximum. A recent  
268 study shows that the isotopic composition of anthropogenic Li in waters can be distinct from that  
269 of natural Li<sup>12</sup>. Thus, further investigation appears necessary to provide a methodology to trace  
270 both Li levels and Li sources (natural or anthropogenic) in the environment.

271

### 272 ***Li biological control***

273 The biological processing of Li in mussels is affected by the Li concentration in the environment  
274 because the mussel-water Li isotope fractionation increases with dissolved Li concentration. The  
275 observed  $^7\text{Li}$  (heavy) enrichment of mussel soft tissue relative to seawater is intriguing as, in  
276 most isotopic systems, biological isotopic fractionation favor light isotopes, mostly because of  
277 kinetic effects during ionic transport. Recent work reveals that Li transport in cells, either passive  
278 or active, is related to a preferential and significant enrichment in  $^6\text{Li}$ <sup>56</sup>. Li has been considered  
279 to be analogous to Na in cells because of the chemical proximity and monovalence of both alkali

280 elements. Indeed, Li is transported by  $\text{Na}^+/\text{H}^+$  ubiquitous exchangers (NHEs), which control  
281 intracellular pH<sup>57-60</sup>. Ca/Na exchangers, likely involved in carbonate shell growth, are also  
282 known to transport Li<sup>61,62</sup>. To verify the potential link between Li, Na, and Ca, we measured  
283 Li/Na and Li/Ca ratios in every individual mussel. Both Li/Na and Li/Ca ratios in mussels are  
284 positively correlated with  $\Delta^7\text{Li}_{\text{mussel-water}}$  (Fig. 3). When the Li/Na and Li/Ca ratios are low, the  
285 observed Li isotopic fractionations are small or negligible ( $\Delta^7\text{Li}_{\text{mussel-water}} \approx 0\text{‰}$ ), whereas the  
286 highest  $\Delta^7\text{Li}_{\text{mussel-water}}$  values correspond to the highest Li/Na and Li/Ca ratios. This result  
287 confirms the biological coupling between Li and Na<sup>63</sup> and suggests that Li transport by NHEs  
288 and Ca/Na transporters are at least partly responsible for the measured Li isotopic compositions.  
289 As Ca is a major building block of bivalve shells, this link might partly explain the vital effects  
290 observed in the Li isotopic signatures of biogenic carbonates<sup>35-38</sup>. Published Li isotopic  
291 compositions of bivalve shells, foraminifera calcite, or corals are scarce, and their interpretation  
292 remains disputed<sup>32,35-38,64</sup>. A physiological control of Li isotopes was suggested by Dellinger *et*  
293 *al.*<sup>35</sup> for various species of molluscs, brachiopods, and echinoderms, and by Vigier *et al.*<sup>38</sup> and  
294 Roberts *et al.*<sup>36</sup> for epibenthic foraminifera. All these studies rely on the Li isotope composition  
295 of the organism's shells, being either calcitic or aragonitic. As a first approximation, we can  
296 compare the mussel soft part  $\delta^7\text{Li}$  values of our CTRL group with those reported for *M. edulis*  
297 shells by Dellinger *et al.*<sup>35</sup>. (Fig. 2B). These shells were collected from mussels living in Cable  
298 Bay (northwest Wales, UK), and have been cultured at different temperatures<sup>65</sup>. They all show  
299  $\delta^7\text{Li}$  values noticeably higher than the  $\delta^7\text{Li}$  values obtained for the soft tissues of our CTRL  
300 group (this study). It is surprising as the formation of calcite induces a significant isotope  
301 fractionation in favor of the  $^6\text{Li}$ <sup>66</sup>. However, both mussel groups do not come from the same  
302 location and it is not known if the seawater in which they were cultured had a seawater-like  $\delta^7\text{Li}$

303 value and Li concentration, or if this seawater was contaminated. Although this comparison  
304 requires more detailed investigations, all of these results suggest that the temporal variations of  
305 ocean Li concentrations may impact both the Li concentrations and the Li isotopic composition  
306 of tissues and shells. Since the isotopic investigation of soft tissues is now technically possible  
307 with high sensitivity mass spectrometer<sup>29</sup>, it appears invaluable to a better understanding of the  
308 vital effects observed in fossils and potentially for refining paleoclimate reconstructions.

309

### 310 *Tracing Li homeostasis and biological thresholds with Li isotopes*

311 In order to bioaccumulate Li as shown in Fig. 2A, the mussel Li excretion flux ( $\Phi_{\text{out}}^{\text{Li}}$ ) must have  
312 been lower than its uptake flux ( $\Phi_{\text{in}}^{\text{Li}}$ ), such that:

$$313 \quad R_f = \frac{f_{\text{out}}^{\text{Li}}}{f_{\text{in}}^{\text{Li}}} < 1 \quad (2)$$

314 As shown in Fig. 2B, and described above, mussel  $\delta^7\text{Li}$  values are systematically higher than  
315 seawater  $\delta^7\text{Li}$  values. However, due to kinetic effects, Li transport through cell membranes is  
316 rather expected to favor the light isotope  $^6\text{Li}^{67}$ . It is common to express these isotope variations  
317 during transport by the isotope fractionation factor ‘ $\alpha$ ’, which is related to the  $\Delta$  notation  
318 (equation 1) using:  $\Delta^7\text{Li} \approx 1,000 \times \ln(\alpha)$ . If both, intake (input) and excretion (output) processes  
319 favor the light ( $^6\text{Li}$ ) isotope, then both  $\alpha_{\text{in}}$  (input) and  $\alpha_{\text{out}}$  (output) are lower than 1 ( $\Delta^7\text{Li} < 0$ ). In  
320 that case, mussel  $^7\text{Li}$  enrichments are possible only if  $^6\text{Li}$  excretion flux is greater than  $^6\text{Li}$  uptake  
321 flux over the experimental duration (i.e., if  $\alpha_{\text{out}} < \alpha_{\text{in}}$ , see Fig. 4 for more details). As the degree  
322 of  $^7\text{Li}$  enrichment is found to increase as a function of the seawater Li concentrations (Fig. 5), the  
323 two possible ways to explain these observations are either that (#1) the ratio between the output



324 and input fractionation factors ( $\alpha_{\text{out}} / \alpha_{\text{oin}}$ ) decreases as a function of seawater Li content, or (#2)  
325 the ratio of the Li output flux to the Li input flux ( $R_{\phi}$ ) increases.

326 Using a simple box model (described in Fig. 4 and in the Supplementary Material), it is possible  
327 to verify more precisely whether the Li regulation in connection to variable Li bioaccumulation  
328 by organisms is compatible with their isotopic compositions. Considering that Li transport is  
329 likely ensured by ubiquitous ion transporters equally present in all *Mytilus edulis* of similar  
330 provenance<sup>57-59</sup>, we assume that all organisms have a similar value for  $\alpha_{\text{out}}$  and  $\alpha_{\text{in}}$ , and therefore  
331 favor hypothesis (#2). With this assumption, and using the equations detailed in the  
332 Supplementary Material, the average mussel  $\delta^7\text{Li}$  value obtained at each condition can be  
333 reproduced within uncertainties (Fig. 5). The calculated input and output Li isotope fractionation  
334 factors,  $\alpha_{\text{in}}$  and  $\alpha_{\text{out}}$ , are 0.999 and 0.989 respectively, and  $R_{\phi}$  is found to increase with increasing  
335 seawater Li concentration, as expected (Table S3).

336 This simple model indicates that, even if mussels bioaccumulate Li, their Li excretion rate  
337 increases significantly as Li contamination increases. This balance between input and output  
338 depends on the seawater Li level and can be related to Li homeostasis, which varies as a function  
339 of Li bioaccumulation, and therefore, of the water contamination. Indeed, the regulation process  
340 of a given element can vary according to low or high accumulation scenario, and be caused, for  
341 example, by an intense elimination process (excretion), or by storage as an internal inert form of  
342 the element (detoxification process).

343 It is possible to investigate further this aspect by exploring the small but significant  $\delta^7\text{Li}_{\text{mussel}}$   
344 variability displayed by individuals from the same experimental group. For each condition,  
345 individual  $\Delta^7\text{Li}_{\text{mussel-water}}$  values correlate linearly with the Li enrichment factor ( $\text{Li}_{\text{m}}/\text{Li}_{\text{sw}}$ , the  
346 ratio of the Li concentrations in the mussels to that in the water, Fig. 6A). These variations are

347 significant, of about 2-3‰ (while the external error on the Li isotope ratio is 1.6‰). For all  
348 individuals,  $Li_m/Li_{sw}$  are higher than 1, which agrees well with the bioaccumulation process  
349 described previously. However, the regressions' slopes in Fig. 6A strongly depend on the  
350 condition. Mussels exposed to low water Li concentrations (i.e. the CTRL and Li-0.5 groups)  
351 display a positive slope, reflecting that  $\Delta^7Li_{mussel-water}$  increases when the individual enrichment  
352 factor increases. On the other hand, mussels exposed to elevated seawater Li concentrations ( $>$   
353  $1\mu g mL^{-1}$ ) (Li-1.0 and Li-1.5 groups) display negative slopes (decreasing  $\Delta^7Li_{mussel-water}$  with the  
354 enrichment factor). There is therefore a Li threshold between 0.5 and  $1\mu g mL^{-1}$ , above which  
355 mussels change their Li biological regulation. Under a significant but limited Li contamination  
356 ( $<1.0\mu g mL^{-1}$ ), the Li excess in the mussel results in a greater Li depuration, which may  
357 correspond to a homeostasis mechanism operating to reduce the Li excess. In contrast, the  
358 negative correlations observed for mussels exposed to seawater Li concentrations  $>0.5\mu g mL^{-1}$   
359 are best explained by a decrease of  $R_\phi$  (Fig. 6A), indicating reduced Li excretion. Under these  
360 conditions, mussels do not - or cannot - entirely eliminate excess Li. This threshold therefore  
361 suggests a physiological shift, and we speculate that it may represent the onset of toxicity that is  
362 the Li concentration beyond which mussels become “stressed”.

363 Major element concentrations in the mussels' soft tissues also support a physiological effect  
364 induced by Li contamination. Indeed, the principal component analysis (PCA, see Methods  
365 section) shows that the essential elements Na, Ca, Fe, and K correlate with each other on the  
366 principal component 1 and are clearly distinct from  $\Delta^7Li_{mussel-water}$ ,  $Li_m$ , and  $Li_{sw}$ , which correlate  
367 on the principal component 2. Figure 6B shows that the “intergroup” variability is discriminated  
368 mostly by  $\Delta^7Li_{mussel-water}$ ,  $Li_m$ , and  $Li_{sw}$ , and therefore depends on the composition and  
369 concentration of environmental Li. On the other hand, the “intragroup” variability is mostly

370 related to variations in essential (major) elements and depends on individual mussel metabolism.  
371 This, altogether with the Li threshold highlighted by Li isotopes, strongly suggests a  
372 physiological effect induced by Li contamination between 500 and 1000  $\mu\text{g L}^{-1}$  (0.5 and 1  $\mu\text{g}$   
373  $\text{mL}^{-1}$ ). Thus, our results demonstrate that, in addition to being a promising new proxy for Li  
374 contamination in coastal ecosystems, mussel Li concentrations and isotopic compositions might  
375 also be used to assess Li toxicity since they respond to mussel adaptation and stress due to high  
376 environmental Li concentrations. Studies on Li accumulation in organisms being at their infancy  
377 and far from being fully understood, further studies would be needed to identify the underlying  
378 regulation mechanisms in mussels facing Li contamination.

379

### 380 *Implications for coastal environments*

381 The highest dissolved Li concentrations ( $>130000 \mu\text{g L}^{-1}$ ) are found in surface waters that drain  
382 the Salars, where Li is mined. Extensive studies of Chilean rivers show that they carry these  
383 elevated Li concentrations down to the western Pacific Ocean. Their dissolved Li concentrations  
384 are several orders of magnitude greater than those of other large rivers, and local estuaries  
385 contain Li concentrations above 1000  $\mu\text{g L}^{-1}$  (100-1000 times more than other estuaries  
386 worldwide). A published compedium<sup>68</sup> shows that marine organisms from the Northern Chilean  
387 littoral display Li concentrations considerably higher than those from other parts of the world -  
388 unrelated to salt flats - such as the French Atlantic coast or the Kerguelen Islands<sup>24</sup>. However, as  
389 discussed in the previous section, Li isotopes indicate that this Li bioaccumulation has a cost  
390 since there is a physiological shift above a threshold between 500 and 1000  $\mu\text{g L}^{-1}$ , which is the  
391 minimum level found in waters of North Chilean estuaries. Li isotope compositions of marine  
392 organisms from natural sites still need to be investigated, but given that the Li transfer to cells is

393 essentially an active process<sup>57</sup>, passing this threshold may trigger abnormal growth patterns due  
394 to chemical stress and damage induced by Li<sup>69</sup>.

395 Overall, these results highlight the need to monitor the evolution of these ‘Li-rich’ ecosystems,  
396 for both their own sustainability, as well as for the local economy and human health. Inhabitants  
397 of the Chilean coast consume 8 to 15 times more seafood and shellfish than inland populations,  
398 while the proportion of other food types such as meat or vegetables are significantly less variable  
399 between the two population groups<sup>68</sup>. This supports the need to quantify and better understand  
400 how these coastal marine organisms bioaccumulate Li. The high Li concentrations measured in  
401 North Chilean shellfish, fish, and drinking waters explain the high Li concentration measured in  
402 the blood (serum), urine, and other tissues collected from the local population<sup>70</sup>. The effects –  
403 negative or positive - of these high Li levels in the diet are less known. Figuorea *et al.*<sup>68</sup>  
404 estimated that the local population eats about 20 g day<sup>-1</sup> of shellfish and seafood. With a Li  
405 concentration of 100 µg g<sup>-1</sup>, as found in local mussels (Table 1), the Li intake is already 2000 µg  
406 day<sup>-1</sup> (twice the dose recommended by Schrauzer<sup>1</sup>). Given that vegetables, cereals, and waters  
407 are also enriched in Li in this area, the Li intake by people living along North Chilean coast is  
408 estimated to be close to the medical dose given to patient treated for neurodegenerative disease  
409 (Table 1).

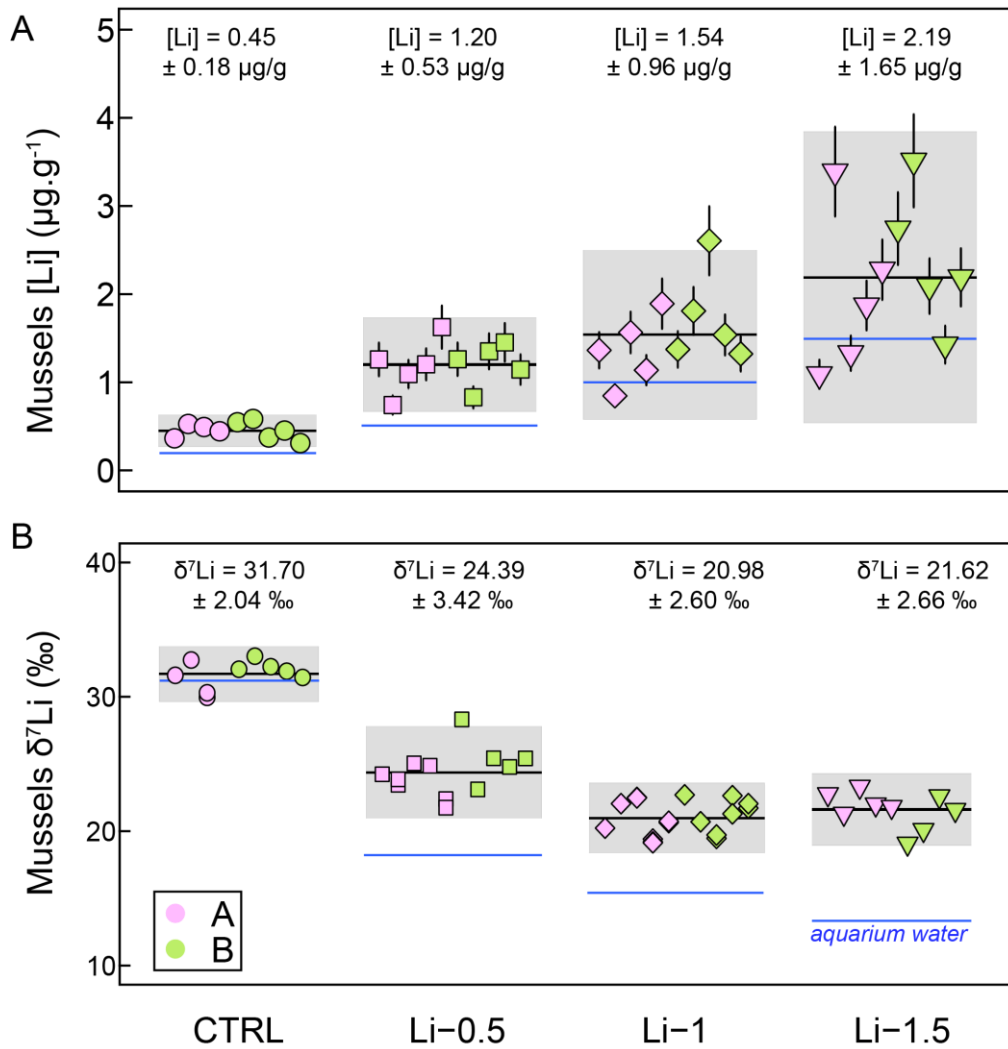
410 In other places in the world, the number of data measured in coastal waters and marine  
411 organisms remains scarce, and it is difficult to estimate the impact of Li mining and  
412 anthropogenic activities at the global scale. A recent study points that Li is not removed during  
413 the waste water treatment plant process<sup>12</sup>. As described in the introduction, a significant level of  
414 Li pollution has been documented in the Han River crossing Seoul<sup>12</sup>. The corresponding Li level  
415 is still low compared to what is contained in North Chilean waters, but the predicted considerable

416 increase of Li production for the next 10 years, along with the development of popular high  
417 technology objects, may significantly increase Li levels in coastal environments if its recycling is  
418 not massively developed.

419

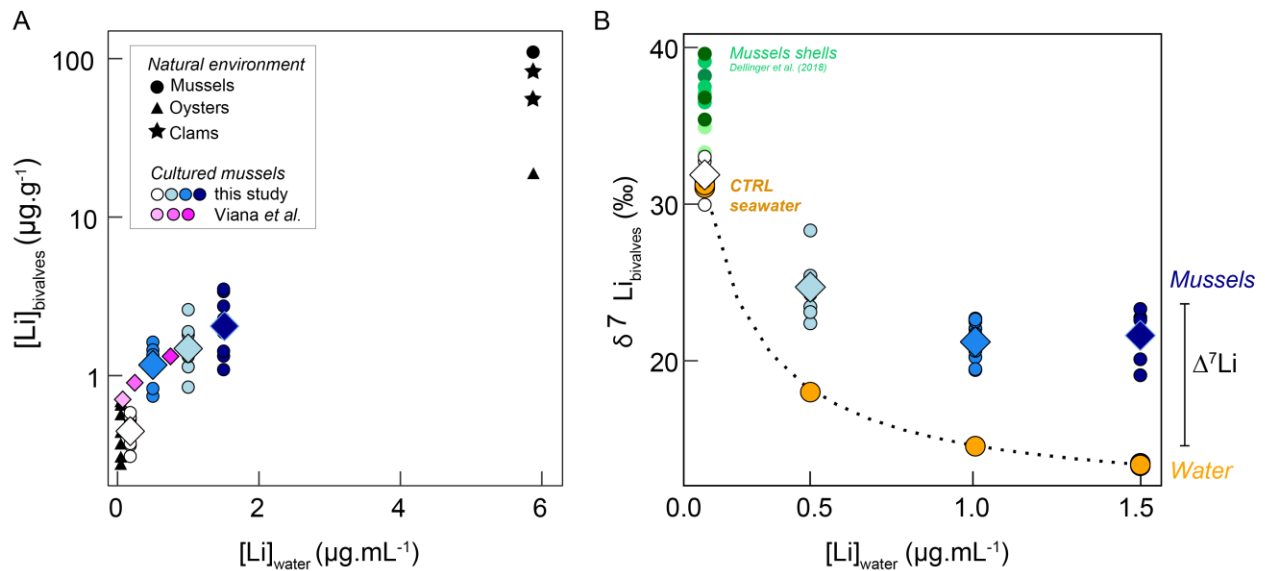
## 420 **Conclusions**

421 This study demonstrates the ability of mussels to bioaccumulate Li, which implies that mussels  
422 may be useful as biomonitoring organisms for Li pollution in coastal water. In addition, we  
423 identify a preferential enrichment of  $^7\text{Li}$  in mussel soft parts. A simple modeling allows us to  
424 relate this Li heavy isotope enrichment to an enhanced NHE activity. Experimental data further  
425 suggests that Li isotopes, more than Li concentrations, are useful to discriminate an organism's  
426 metabolic or physiological threshold when facing high contaminant level in the environment.  
427 Combined with ancillary environmental data, our experimental results have profound  
428 implications for the fate of coastal ecosystems and shellfish consumption by population living in  
429 high environmental Li regions. Finally, they also clarify how biological activity can impact the  
430 Li isotope compositions measured in calcitic shells and may bias the record of past ocean  
431 variations.

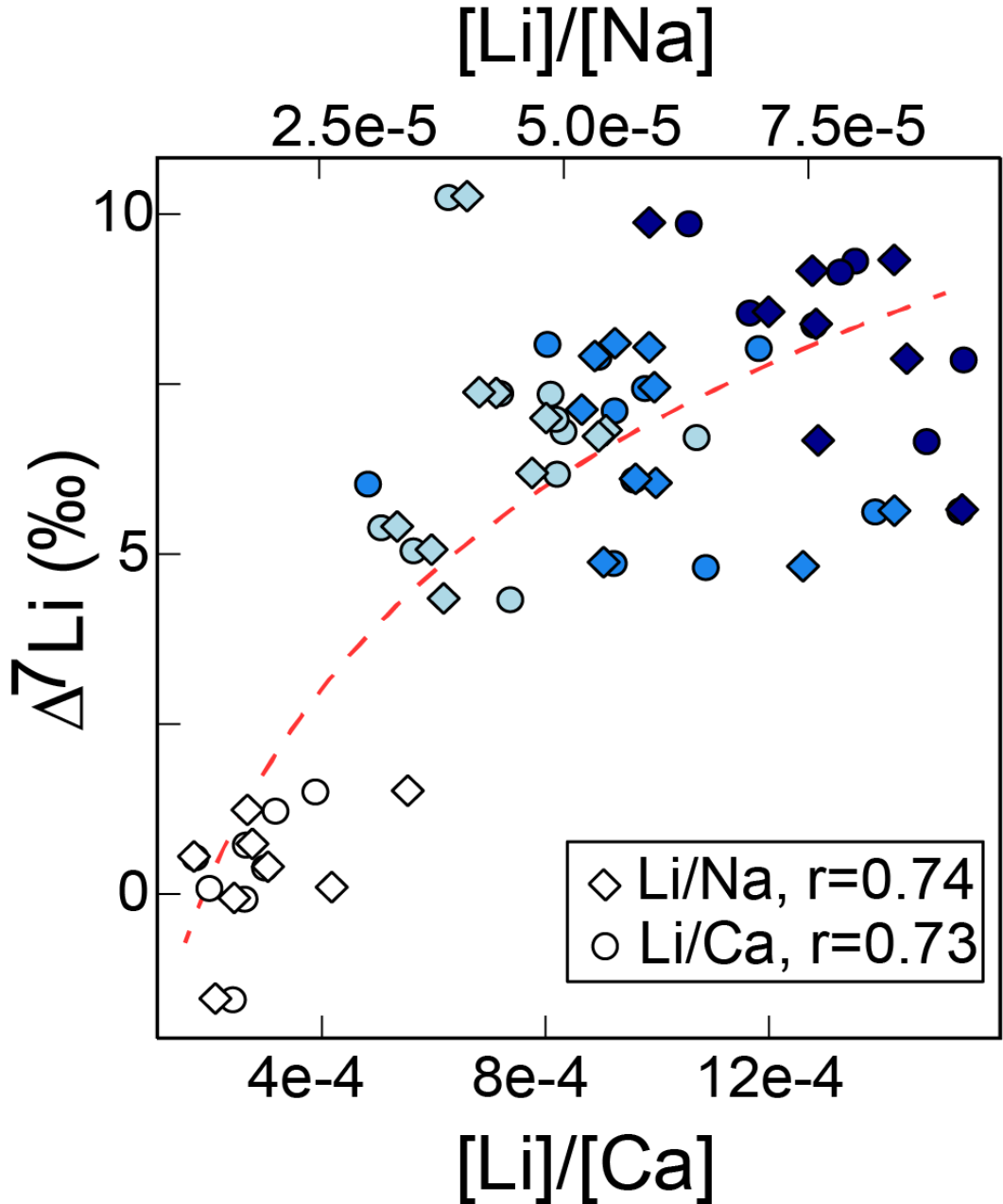


432

433 **Figure 1:** Li concentrations ( $[Li]$ ) and isotopic compositions ( $\delta^7Li$ ) of mussel soft tissues as a  
 434 function of water Li level. Blue mussels were exposed during 4 days to seawater with  $[Li] = 0.18$   
 435  $\mu\text{g mL}^{-1}$  (natural seawater, control group CTRL),  $0.5 \mu\text{g mL}^{-1}$  (Li-0.5),  $1.0 \mu\text{g mL}^{-1}$  (Li-1.0), or  
 436  $1.5 \mu\text{g mL}^{-1}$  (Li-1.5). A (pink) and B (green) are the two experimental replicates. Reported errors  
 437 are  $\pm 2SD$  ( $n = 10$  for Li-0.5, Li-1.0, and Li 1.5;  $n = 9$  for CTRL). Replicates A and B display the  
 438 same average values (Wilcoxon test,  $p > 0.05$ ), within uncertainties. The seawater in each  
 439 experimental group is characterized by a distinct but constant  $\delta^7Li$  (blue lines). **(A)** The  
 440 variability of mussel Li concentrations increases from 44%(CTRL) to 75% (Li\_1.5).



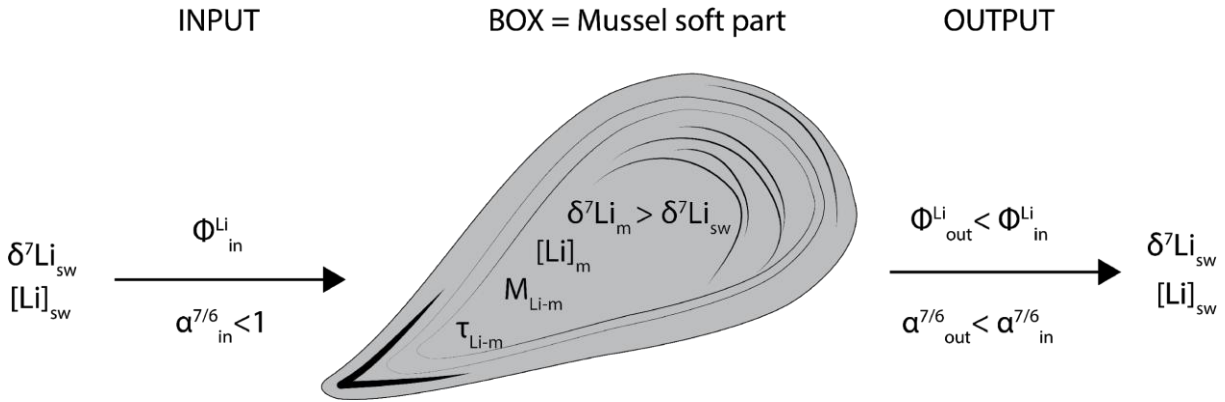
441  
 442 **Figure 2:** Observed Li bioconcentration and Li isotopic fractionation displayed by blue mussels  
 443 as a function of seawater Li concentration. **(A)** Mussel Li concentrations: circles and diamonds  
 444 indicate individual analyses and average values per experimental group, respectively. Black  
 445 symbols are for bivalves collected in their natural environment (the Bay of Biscay for those at  
 446  $0.18 \mu g mL^{-1} [Li]_{water}^{24}$ , and Rio Camarones in Chile for those at  $6 \mu g mL^{-1} [Li]_{water}^{68}$ ). Blue  
 447 tones symbol color indicates experimental group (i.e., Li concentration in seawater): white,  
 448 CTRL,  $0.18 \mu g Li mL^{-1}$ ; light blue, Li-0.5,  $0.5 \mu g Li mL^{-1}$ ; blue, Li-1.0,  $1.0 \mu g Li mL^{-1}$ ; and  
 449 dark blue, Li-1.5,  $1.5 \mu g Li mL^{-1}$ . Pink tones symbol color are from Viana et al.<sup>71</sup> (long-term Li  
 450 exposure experiment). **(B)** Mussel (symbols as in (A)) and water Li isotopic compositions  
 451 (orange circles). The dotted line shows the binary mixing curve between natural filtered seawater  
 452 ( $\delta^7 Li = 31.2‰$ ) and the Li spike used in the experiment ( $\delta^7 Li = 10.8‰$ ). For comparison, Li  
 453 isotopic compositions of *Mytilus eduli* calcite shells collected in Cable Bay, UK, are also  
 454 reported in green (data from Freitas *et al.*<sup>65</sup> and Dellinger *et al.*<sup>35</sup>). These mussels were bred at  
 455 different water temperature from 11 to 20°C, represented by the pale to dark green gradient. The  
 456 Li concentration and  $\delta^7 Li$  value of the seawater in which they grew is not known.



457

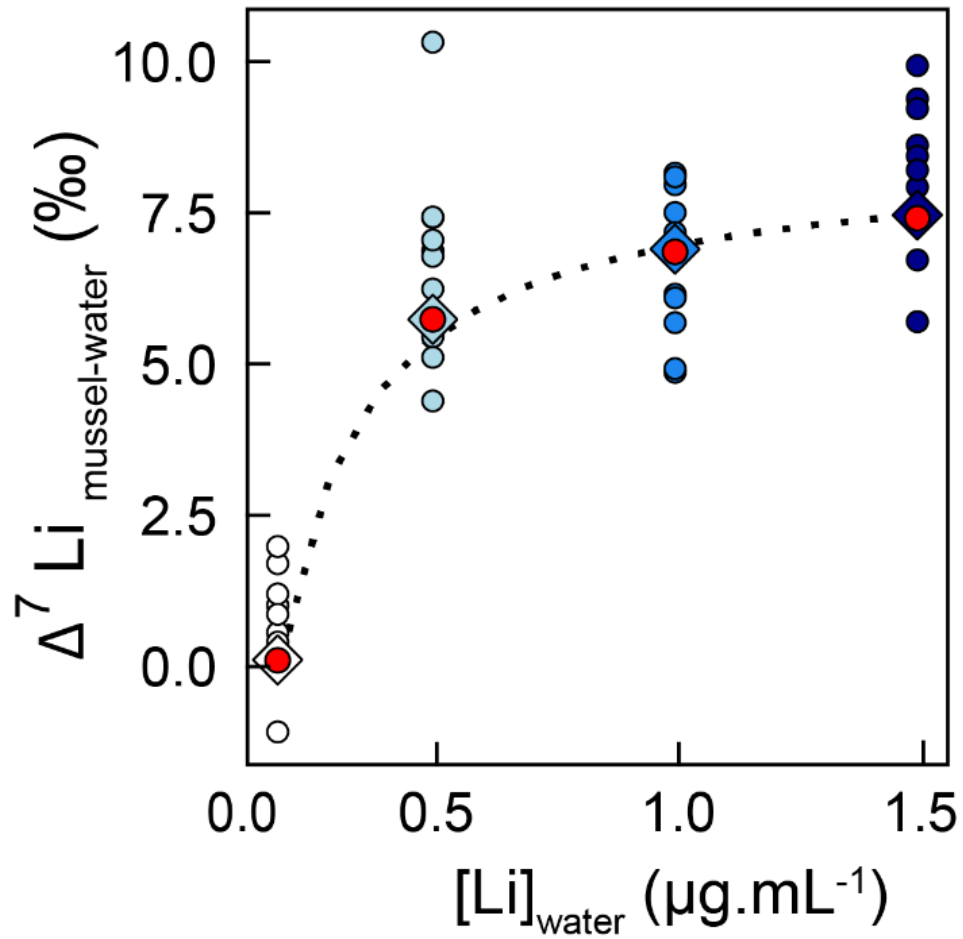
458 **Figure 3:** The effect of biological processing on mussel Li isotopic fractionations.  $\Delta^7\text{Li}_{\text{mussel-water}}$   
 459 values determined in this study (symbol colors as in Fig. 2) as a function of Li/Ca (circles) and  
 460 Li/Na (diamonds) ratios in mussels. The red dashed line is the empirical positive correlation  
 461 between both parameters ( $r$ =correlation coefficients). The Ca/Na ratios measured in mussels  
 462 display a restricted range, on average  $0.06 \pm 0.02$  (SD,  $n = 38$ ).





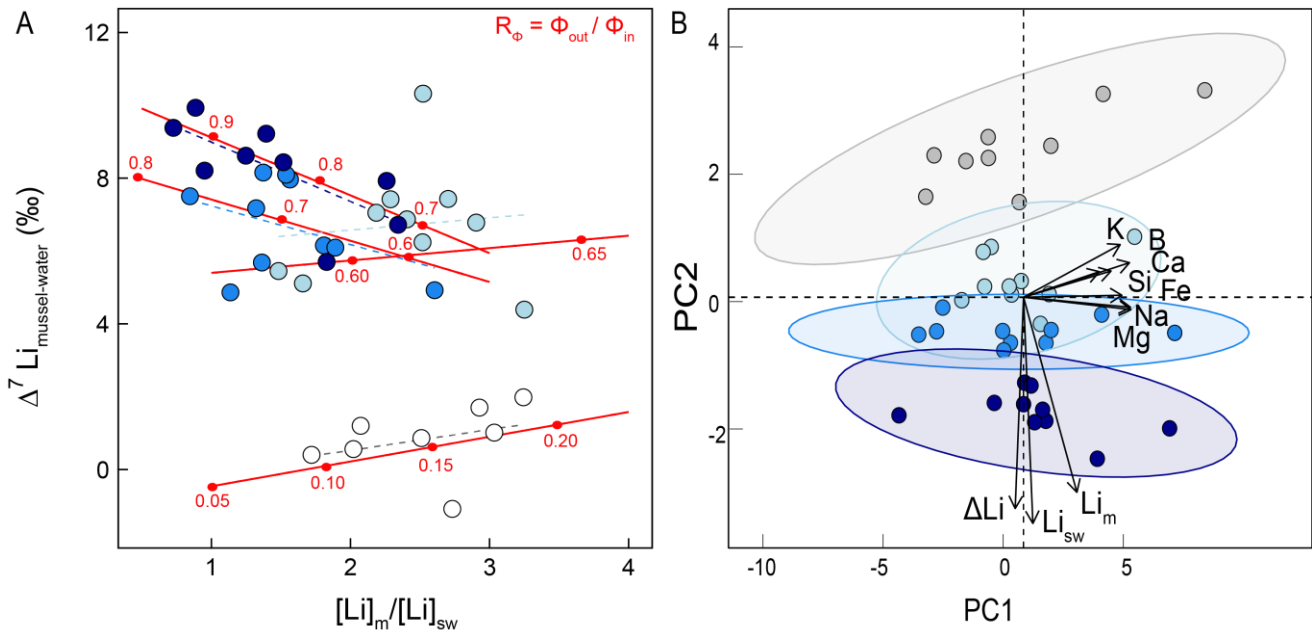
463

464 **Figure 4:** Box model of Li isotope composition in mussel soft tissue. Variables are: [Li], Li  
 465 concentration ( $\mu\text{g g}^{-1}$  or  $\mu\text{g mL}^{-1}$ );  $M_{\text{Li}}$ , Li mass ( $\mu\text{g}$ );  $\delta^7\text{Li}$ , Li isotopic composition (‰);  $\tau_{\text{Li}}$ , Li  
 466 residence time (d);  $\alpha$ , Li isotopic fractionation factor between mussel and water;  $\alpha =$   
 467  $(^7\text{Li}/^6\text{Li})_{\text{mussel}} / (^7\text{Li}/^6\text{Li})_{\text{water}}$ , which relates to  $\Delta^7\text{Li}$  as:  $\Delta^7\text{Li}_{\text{mussel-water}} = \delta^7\text{Li}_{\text{mussel}} - \delta^7\text{Li}_{\text{water}} \approx 1,000$   
 468  $\times \ln(\alpha)$ ;  $\alpha_{\text{in}}$  and  $\alpha_{\text{out}}$  represent the magnitude of Li isotopic fractionations during uptake and  
 469 excretion, respectively; and  $\phi_{\text{Li}}$ , Li flux ( $\mu\text{g d}^{-1}$ ). Subscripts are: m, mussel; sw, seawater; in,  
 470 input; and out, output. Using the equations developed in the Supplementary Material, the best  
 471 average  $\delta^7\text{Li}_{\text{m-mod}}$  values (i.e., modeled  $\delta^7\text{Li}_{\text{mussel}}$  values) for each experimental condition were  
 472 determined by minimizing the difference between the modeled and measured  $\delta^7\text{Li}$  values (i.e.,  
 473  $\delta^7\text{Li}_{\text{m-mod}} - \delta^7\text{Li}_{\text{m-meas}}$ ), with  $\alpha_{\text{out}}$  and  $\alpha_{\text{in}}$  ranging between 0.9 and 1.



474

475 **Figure 5:** Observed and modeled Li isotopic fractionations in mussels as a function of seawater  
 476 Li level. Individual (circles) and average  $\Delta^7\text{Li}_{\text{mussel-water}}$  values (diamonds) are reported for the  
 477 four experimental conditions. Red circles display the modeled isotope fractionations calculated  
 478 by the box model detailed in the text and in the Supplementary Material.



479

480 **Figure 6:** The controls of Li excretion/intake rate and of essential elements on mussel-water Li

481 isotopic fractionation. **(A)**  $\Delta^7Li_{mussel-water}$  vs. Li enrichment factor (i.e., the ratio of the Li

482 concentration in mussels to that in water, equivalent to the bioaccumulation factor or partition

483 coefficient between mussels and seawater). Symbol colors indicate the experimental conditions

484 as in Fig. 2. Solid lines are intragroup linear regressions. Mussels exposed to relatively Li-poor

485 conditions (CTRL and Li-0.5 groups) show positive slopes, whereas those exposed to Li-rich

486 conditions (Li-1.0 and Li-1.5 groups) define negative slopes. Red lines display model variations

487 and red dots indicate specific  $R_\phi$  values. **(B)** Principal component analysis (PCA) of all mussels

488 (symbols as in (A), shaded ellipses represent intragroup variability). PC1 and PC2 are principal

489 components 1 and 2. Arrow length is proportional to the percentage contribution of these first

490 two principal components to the observed variation of each variable. PC1 and PC2 represent

491 75% of the variability in the dataset. Variables can be separated into three groups: mussel B, Ca,

492 Fe, K, Mg, Na, and Si concentrations on PC1 and  $\Delta^7Li_{mussel-water}$ ,  $Li_m$ , and  $Li_{sw}$  on PC2.

**Table 1:** Compilation of Li concentrations and fluxes estimated for several contexts.

	Sample type	Location and information	Li concentration	Unit	Reference
<b>Environments</b>	Salar draining waters	Chile - Atacama	130000 - 1240000	µg Li/L	BRGM <sup>8</sup>
		Argentina	600000	µg Li/L	BRGM <sup>8</sup>
	Geothermal fluids	W USA	200000	µg Li/L	BRGM <sup>8</sup>
		Italy	480000	µg Li/L	BRGM <sup>8</sup>
		Mid-oceanic ridges	1000-10000	µg Li/L	Verney-Carron et al., 2015 <sup>72</sup>
	Seawater	Pelagic	180	µg Li/L	Broecker, 1982 <sup>73</sup>
	Large rivers	Global scale	0.1 - 5	µg Li/L	Huh et al., 1998 <sup>74</sup>
	Chilean river and tap waters	Azapa, Rio San Jose	90 - 160	µg Li/L	Figueroa et al., 2012 <sup>7</sup>
		Lluta, Lauca Altiplano	60 - 1830	µg Li/L	Figueroa et al., 2012 <sup>7</sup>
		Camarones	400 - 5600	µg Li/L	Figueroa et al., 2012 <sup>7</sup>
		Lauca, Rio Tignamar	20 - 450	µg Li/L	Figueroa et al., 2012 <sup>7</sup>
		Rio Loa, Salado	1200 - 7700	µg Li/L	Figueroa et al., 2012 <sup>7</sup>
		Atacama	300 - 2570	µg Li/L	Figueroa et al., 2012 <sup>7</sup>
	Chilean estuaries	Lluta estuary	1300 - 1580	µg Li/L	Figueroa et al., 2012 <sup>7</sup>
		Camarones estuary	3500 - 7600	µg Li/L	Figueroa et al., 2012 <sup>7</sup>
	Urban river	S Korea - Seoul	0.3 - 1.7	µg Li/L	Choi et al., 2019 <sup>12</sup>
Wastewaters	S Korea - Seoul	1 - 5	µg Li/L	Choi et al., 2019 <sup>12</sup>	
	S Korea - Seoul	0.3 - 0.7	µg Li/L	Choi et al., 2019 <sup>12</sup>	
Tap water	Peru - Lima airport	115	µg Li/L	Figueroa et al., 2012 <sup>7</sup>	
	Peru - Pachia	144	µg Li/L	Figueroa et al., 2012 <sup>7</sup>	
	Peru - Pocolla	83	µg Li/L	Figueroa et al., 2012 <sup>7</sup>	
Mineral waters	Germany	1.7 - 1724	µg Li/L	Seidel et al., 2019 <sup>75</sup>	
Drinking waters close to Salar	Australia, Chile, Argentina, Bolivia	>1000	µg Li/L	Seidel et al., 2019 <sup>75</sup>	
<b>Humans</b>	Serum	Germany / N Chile	0.03-175	µg Li/L	Seidel et al., 2019 <sup>75</sup> , Figueroa et al., 2014 <sup>70</sup>
	Blood		<60	µg Li/L	BRGM <sup>8</sup>
	24h Urine	Germany	21 - 1172	µg Li/L	Seidel et al., 2019 <sup>75</sup>
	Urine	N Chile	140 - 5800	µg Li/L	Figueroa et al., 2014 <sup>70</sup>
	Toxic threshold in plasma		10000	µg Li/L	Aral and Vecchio-Sadus, 2008 <sup>4</sup>
	Lethal threshold in plasma		20000	µg Li/L	Aral and Vecchio-Sadus, 2008 <sup>4</sup>
	Fluxes	Provisory intake recommended by some	1000	µg Li /day	Schrauzer, 2002 <sup>1</sup>
Li drug (bipolarity)		500000 - 2000000	µg Li/day	Young, 2009 <sup>76</sup>	
Microdose affecting Alzheimer patients		300	µg Li /day	Andrade Nunes et al., 2013 <sup>77</sup>	
Li intake by N Chile inhabitants		5000 - 50000	µg Li /day	Figueroa et al., 2013 <sup>68</sup>	
<b>Marine organisms</b>	Tunicates	N Chile - Piure - Coastal Shellfish	33	µg Li/g	Figueroa et al., 2013 <sup>68</sup>
		Atlantic, Pacific	0.05 - 0.8	µg Li/g	Thibon, Weppe et al., 2020 <sup>24</sup>
	Bivalves	N Chile - Oyster - Coastal Shellfish	19	µg Li/g	Figueroa et al., 2013 <sup>68</sup>
		N Chile - Clam - Coastal Shellfish	53-83	µg Li/g	Figueroa et al., 2013 <sup>68</sup>
		N Chile - Mussel - Coastal Shellfish	111	µg Li/g	Figueroa et al., 2013 <sup>68</sup>
	Cephalopods	Atlantic, Pacific, Indian ocean	0.05 - 0.2	µg Li/g	Thibon, Weppe et al., 2020 <sup>24</sup>
	Gastropods	N Chile - Abalone - Coastal Shellfish	20	µg Li/g	Figueroa et al., 2013 <sup>68</sup>
		N Chile - Limpet - Coastal Shellfish	85	µg Li/g	Figueroa et al., 2013 <sup>68</sup>
	Crustaceans	Atlantic, Pacific	0.1 - 0.3	µg Li/g	Thibon, Weppe et al., 2020 <sup>24</sup>
	Fish	Atlantic, Pacific, Indian ocean	0.03 - 0.5	µg Li/g	Thibon, Weppe et al., 2020 <sup>24</sup>
N Chile - Frog fish		18	µg Li/g	Figueroa et al., 2013 <sup>68</sup>	
N Chile - Barred Hogfish		20	µg Li/g	Figueroa et al., 2013 <sup>68</sup>	
N Chile - Bass		25	µg Li/g	Figueroa et al., 2013 <sup>68</sup>	
N Chile - Flounder		51	µg Li/g	Figueroa et al., 2013 <sup>68</sup>	
N Chile - Shark		68	µg Li/g	Figueroa et al., 2013 <sup>68</sup>	
N Chile - H macrophthalmos		86	µg Li/g	Figueroa et al., 2013 <sup>68</sup>	
N Chile - White seabream		99	µg Li/g	Figueroa et al., 2013 <sup>68</sup>	
N Chile - John Dory		103	µg Li/g	Figueroa et al., 2013 <sup>68</sup>	

495 ASSOCIATED CONTENT

496 **Supporting Information.**

497 Supplementary Material is available and contents supplementary figures, data tables, and box  
498 model equations.

499

500

501 AUTHOR INFORMATION

502 **Corresponding Author**

503 \*fanny.thibon@osb-vlfr.fr

504 **Author Contributions**

505 N. Vigier and M. Metian led the project. F. Oberhänsli, E. Vassileva, and A.M. Orani performed  
506 sample preparation and Li concentration measurements. M. Montanes, N. Vigier, and P. Telouk  
507 performed the sample Li purification and Li isotopic ratio measurements. F. Thibon modeled the  
508 data and wrote the original draft of the manuscript. F. Thibon, N. Vigier, M. Metian, and P.  
509 Swarzenski contributed to review and editing the manuscript. All authors have given approval to  
510 the final version of the manuscript.

511

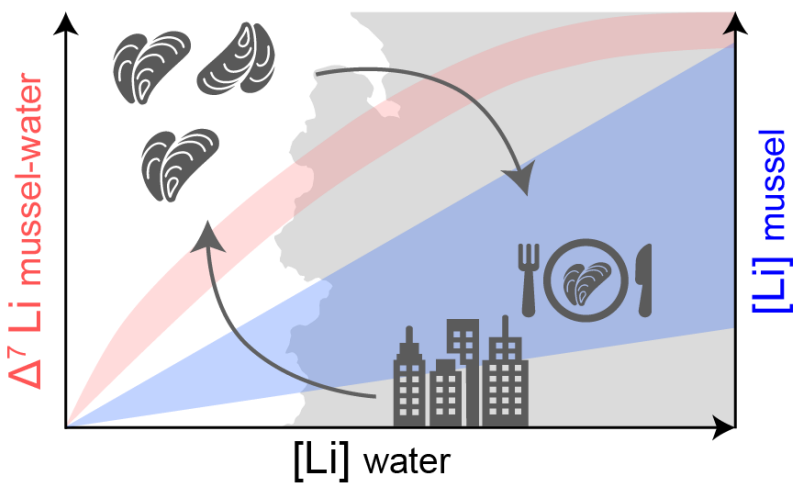
512 ACKNOWLEDGMENT

513 We acknowledge financial support from the ANR ISO2MET ([//anr.fr/Projet-ANR-18-CE34-](http://anr.fr/Projet-ANR-18-CE34-0002)  
514 [0002; www.iso2met-project.fr/](http://www.iso2met-project.fr/)) and access to facilities provided by the International Atomic  
515 Energy Agency (IAEA) of Monaco and the CNRS-INSU at ENS-Lyon. The IAEA is grateful for

516 the support provided to its Environment Laboratories by the Government of the Principality of  
517 Monaco. We also thank a lot Steeve Comeau for his help reworking this manuscript.

518

519 TOC GRAPHIC



520

521 REFERENCES

522

523 (1) Schrauzer, G. N. Lithium: Occurrence, Dietary Intakes, Nutritional Essentiality. *Journal of the*  
524 *American College of Nutrition* **2002**, *21* (1), 14–21.  
525 <https://doi.org/10.1080/07315724.2002.10719188>.

526 (2) Egorova, K. S.; Ananikov, V. P. Toxicity of Metal Compounds: Knowledge and Myths.  
527 *Organometallics* **2017**, *36* (21), 4071–4090. <https://doi.org/10.1021/acs.organomet.7b00605>.

528 (3) Zoroddu, M. A.; Aaseth, J.; Crisponi, G.; Medici, S.; Peana, M.; Nurchi, V. M. The Essential Metals  
529 for Humans: A Brief Overview. *Journal of Inorganic Biochemistry* **2019**, *195*, 120–129.  
530 <https://doi.org/10.1016/j.jinorgbio.2019.03.013>.

531 (4) Aral, H.; Vecchio-Sadus, A. Toxicity of Lithium to Humans and the Environment—A Literature  
532 Review. *Ecotoxicology and Environmental Safety* **2008**, *70* (3), 349–356.  
533 <https://doi.org/10.1016/j.ecoenv.2008.02.026>.

534 (5) Timmer, R. T.; Sands, J. M. Lithium Intoxication. *Journal of the American Society of Nephrology*  
535 **1999**, *10* (3), 666–674.

536 (6) Schou, M.; Amdisen, A.; Trap-Jensen, J. Lithium Poisoning. *American Journal of Psychiatry* **1968**,  
537 *125* (4), 520–527. <https://doi.org/10.1176/ajp.125.4.520>.

538 (7) Figueroa, L.; Barton, S.; Schull, W.; Razmilic, B.; Zumaeta, O.; Young, A.; Kamiya, Y.; Hoskins, J.;  
539 Ilgren, E. Environmental Lithium Exposure in the North of Chile--I. Natural Water Sources.  
540 *Biological Trace Element Research* **2012**, *149* (2), 280–290. [https://doi.org/10.1007/s12011-012-](https://doi.org/10.1007/s12011-012-9417-6)  
541 [9417-6](https://doi.org/10.1007/s12011-012-9417-6).

542 (8) Labbé, J. F.; Daw, G. Panorama 2011 Du Marché Du Lithium. *BRGM* **2012**.

543 (9) Leguériel, M.; Lefebvre, G.; Christmann, P. Compétition Entre Secteurs Industriels Pour l'accès  
544 Aux Matières Premières, 2018.

- 545 (10) Mohr, S. H.; Mudd, G. M.; Giurco, D. Lithium Resources and Production: Critical Assessment and  
546 Global Projections. *Minerals* **2012**, *2* (1), 65–84. <https://doi.org/10.3390/min2010065>.
- 547 (11) Kszos, L. A.; Stewart, A. J. Review of Lithium in the Aquatic Environment: Distribution in the  
548 United States, Toxicity and Case Example of Groundwater Contamination. *Ecotoxicology* **2003**, *12*  
549 (5), 439–447. <https://doi.org/10.1023/a:1026112507664>.
- 550 (12) Choi, H.-B.; Ryu, J.-S.; Shin, W.-J.; Vigier, N. The Impact of Anthropogenic Inputs on Lithium  
551 Content in River and Tap Water. *Nature Communications* **2019**, *10* (1), 5371.  
552 <https://doi.org/10.1038/s41467-019-13376-y>.
- 553 (13) Decarreau, A.; Vigier, N.; Pálková, H.; Petit, S.; Vieillard, P.; Fontaine, C. Partitioning of Lithium  
554 between Smectite and Solution: An Experimental Approach. *Geochimica et Cosmochimica Acta*  
555 **2012**, *85*, 314–325.
- 556 (14) Schwab, A. B.; O’Connell, M. E.; Long, S. E. The Use of Lithium Concentration Data and Isotopic  
557 Ratios as Hydrologic Tracers in a First-Order Catchment. *Geol Soc Am Prog Abst* **1995**, *27*, A97.
- 558 (15) Hogan, J. F.; Blum, J. D. Boron and Lithium Isotopes as Groundwater Tracers: A Study at the Fresh  
559 Kills Landfill, Staten Island, New York, USA. *Applied Geochemistry* **2003**, *18* (4), 615–627.  
560 [https://doi.org/10.1016/S0883-2927\(02\)00153-1](https://doi.org/10.1016/S0883-2927(02)00153-1).
- 561 (16) Pogge von Strandmann, P. A. E.; Burton, K. W.; James, R. H.; van Calsteren, P.; Gíslason, S. R.;  
562 Mokadem, F. Riverine Behaviour of Uranium and Lithium Isotopes in an Actively Glaciated  
563 Basaltic Terrain. *Earth and Planetary Science Letters* **2006**, *251* (1), 134–147.  
564 <https://doi.org/10.1016/j.epsl.2006.09.001>.
- 565 (17) Yang, C.; Yang, S.; Vigier, N.; Lian, E.; Lai, Z. Behavior of Li Isotopes along a 2D Transect in the  
566 Changjiang (Yangtze) Estuary. *Earth and Planetary Science Letters*. submitted.



- 567 (18) Phillips, D. J. H. The Common Mussel *Mytilus Edulis* as an Indicator of Pollution by Zinc, Cadmium,  
568 Lead and Copper. I. Effects of Environmental Variables on Uptake of Metals. *Marine Biology* **1976**,  
569 *38* (1), 59–69. <https://doi.org/10.1007/bf00391486>.
- 570 (19) Shi, D.; Wang, W.-X. Modification of Trace Metal Accumulation in the Green Mussel *Perna Viridis*  
571 by Exposure to Ag, Cu, and Zn. *Environmental Pollution* **2004**, *132* (2), 265–277.  
572 <https://doi.org/10.1016/j.envpol.2004.04.023>.
- 573 (20) Viarengo, A.; Canesi, L. Mussels as Biological Indicators of Pollution. *Aquaculture* **1991**, *94* (2),  
574 225–243. [https://doi.org/10.1016/0044-8486\(91\)90120-V](https://doi.org/10.1016/0044-8486(91)90120-V).
- 575 (21) Claisse, D.; Arnold, M.; Jean-Yves, Q. Le Réseau National d’observation de La Qualité Du Milieu  
576 Marin (RNO). *Analisis Magazine* **1992**, *20* (6), 19–22.
- 577 (22) Goldberg, E. The Mussel Watch - A First Step in Global Marine Monitoring. *Marine Pollution*  
578 *Bulletin* **1975**, *6*, 111–111. [https://doi.org/10.1016/0025-326x\(75\)90271-4](https://doi.org/10.1016/0025-326x(75)90271-4).
- 579 (23) Kimbrough, K. L.; Lauenstein, G.; Christensen, J.; Apeti, D. An Assessment of Two Decades of  
580 Contaminant Monitoring in the Nation’s Coastal Zone. **2008**.
- 581 (24) Thibon, F.; Weppe, L.; Vigier, N.; Churlaud, C.; Lacoue-Labarthe, T.; Metian, M.; Cherel, Y.;  
582 Bustamante, P. Large-Scale Survey of Lithium Concentrations in Marine Organisms. *Science of The*  
583 *Total Environment* **2021**, *751*, 141453. <https://doi.org/10.1016/j.scitotenv.2020.141453>.
- 584 (25) Albarède, F. Metal Stable Isotopes in the Human Body: A Tribute of Geochemistry to Medicine.  
585 *Elements* **2015**, *11* (4), 265–269. <https://doi.org/10.2113/gselements.11.4.265>.
- 586 (26) Balter, V.; da Costa, A. N.; Bondanese, V. P.; Jaouen, K.; Lamboux, A.; Sangrajrang, S.; Vincent, N.;  
587 Fourel, F.; Télouk, P.; Gigou, M. Natural Variations of Copper and Sulfur Stable Isotopes in Blood  
588 of Hepatocellular Carcinoma Patients. *Proceedings of the National Academy of Sciences* **2015**, *112*  
589 (4), 982–985.

- 590 (27) Costas-Rodríguez, M.; Delanghe, J.; Vanhaecke, F. High-Precision Isotopic Analysis of Essential  
591 Mineral Elements in Biomedicine: Natural Isotope Ratio Variations as Potential Diagnostic and/or  
592 Prognostic Markers. *Trends in Analytical Chemistry* **2016**, *76*, 182–193.  
593 <https://doi.org/10.1016/j.trac.2015.10.008>.
- 594 (28) Vanhaecke, F.; Costas-Rodríguez, M. What's up Doc? - High-Precision Isotopic Analysis of  
595 Essential Metals in Biofluids for Medical Diagnosis. *spectroscopyeurope* **2015**, *27* (3), 11–14.
- 596 (29) Balter, V.; Vigier, N. Natural Variations of Lithium Isotopes in a Mammalian Model. *Metallomics*  
597 **2014**, *6* (3), 582–586.
- 598 (30) Hathorne, E. C.; James, R. H. Temporal Record of Lithium in Seawater: A Tracer for Silicate  
599 Weathering? *Earth and Planetary Science Letters* **2006**, *246* (3–4), 393–406.  
600 <https://doi.org/10.1016/j.epsl.2006.04.020>.
- 601 (31) Li, G.; West, A. J. Evolution of Cenozoic Seawater Lithium Isotopes: Coupling of Global Denudation  
602 Regime and Shifting Seawater Sinks. *Earth and Planetary Science Letters* **2014**, *401*, 284–293.  
603 <https://doi.org/10.1016/j.epsl.2014.06.011>.
- 604 (32) Misra, S.; Froelich, P. N. Lithium Isotope History of Cenozoic Seawater: Changes in Silicate  
605 Weathering and Reverse Weathering. *Science* **2012**, *335* (6070), 818–823.  
606 <https://doi.org/10.1126/science.1214697>.
- 607 (33) Vigier, N.; Godderis, Y. A New Approach for Modeling the Cenozoic Oceanic Lithium Isotope  
608 Paleo-Variations: The Key Role of Climate. *Climate of the Past Discussions* **2014**, *10* (4).  
609 <https://doi.org/10.5194/cp-11-635-2015>.
- 610 (34) Wanner, C.; Sonnenthal, E. L.; Liu, X.-M. Seawater  $\delta^7\text{Li}$ : A Direct Proxy for Global  $\text{CO}_2$   
611 Consumption by Continental Silicate Weathering? *Chemical geology* **2014**, *381*, 154–167.  
612 <https://doi.org/10.1016/j.chemgeo.2014.05.005>.

- 613 (35) Dellinger, M.; West, A. J.; Paris, G.; Adkins, J. F.; Pogge von Strandmann, P. A. E.; Ullmann, C. V.;  
614 Eagle, R. A.; Freitas, P.; Bagard, M.-L.; Ries, J. B.; Corsetti, F. A.; Perez-Huerta, A.; Kampf, A. R. The  
615 Li Isotope Composition of Marine Biogenic Carbonates: Patterns and Mechanisms. *Geochimica et*  
616 *Cosmochimica Acta* **2018**, *236*, 315–335. <https://doi.org/10.1016/j.gca.2018.03.014>.
- 617 (36) Roberts, J.; Kaczmarek, K.; Langer, G.; Skinner, L.; Bijma, J.; Bradbury, H.; Turchyn, A.; Lamy, F.;  
618 Misra, S. Lithium Isotopic Composition of Benthic Foraminifera: A New Proxy for Paleo-PH  
619 Reconstruction. *Geochimica et Cosmochimica Acta* **2018**, *236*, 336–350.  
620 <https://doi.org/10.1016/j.gca.2018.02.038>.
- 621 (37) Thébault, J.; Chauvaud, L. Li/Ca Enrichments in Great Scallop Shells (*Pecten Maximus*) and Their  
622 Relationship with Phytoplankton Blooms. *Palaeogeography, Palaeoclimatology, Palaeoecology*  
623 **2012**, *373*, 108–122. <https://doi.org/10.1016/j.palaeo.2011.12.014>.
- 624 (38) Vigier, N.; Rollion-Bard, C.; Levenson, Y.; Erez, J. Lithium Isotopes in Foraminifera Shells as a Novel  
625 Proxy for the Ocean Dissolved Inorganic Carbon (DIC). *Comptes Rendus Geoscience* **2015**, *347* (1),  
626 43–51. <https://doi.org/10.1016/j.crte.2014.12.001>.
- 627 (39) Pogge von Strandmann, P. A. E.; Jenkyns, H. C.; Woodfine, R. G. Lithium Isotope Evidence for  
628 Enhanced Weathering during Oceanic Anoxic Event 2. *Nature Geoscience* **2013**, *6* (8), 668–672.  
629 <https://doi.org/10.1038/ngeo1875>.
- 630 (40) Sezer, N.; Kılıç, Ö.; Metian, M.; Belivermiş, M. Effects of Ocean Acidification on <sup>109</sup>Cd, <sup>57</sup>Co, and  
631 <sup>134</sup>Cs Bioconcentration by the European Oyster (*Ostrea Edulis*): Biokinetics and Tissue-to-  
632 Subcellular Partitioning. *Journal of Environmental Radioactivity* **2018**, *192*, 376–384.  
633 <https://doi.org/10.1016/j.jenvrad.2018.07.011>.
- 634 (41) Metian, M.; Pouil, S.; Hédouin, L.; Oberhänsli, F.; Teyssié, J.-L.; Bustamante, P.; Warnau, M.  
635 Differential Bioaccumulation of <sup>134</sup>Cs in Tropical Marine Organisms and the Relative Importance

- 636 of Exposure Pathways. *Journal of Environmental Radioactivity* **2016**, *152*, 127–135.  
637 <https://doi.org/10.1016/j.jenvrad.2015.11.012>.
- 638 (42) Metian, M.; Warnau, M.; Teyssié, J.-L.; Bustamante, P. Characterization of <sup>241</sup>Am and <sup>134</sup>Cs  
639 Bioaccumulation in the King Scallop *Pecten Maximus*: Investigation via Three Exposure Pathways.  
640 *Journal of Environmental Radioactivity* **2011**, *102* (6), 543–550.  
641 <https://doi.org/10.1016/j.jenvrad.2011.02.008>.
- 642 (43) Nagato, E. G.; D’eon, J. C.; Lankadurai, B. P.; Poirier, D. G.; Reiner, E. J.; Simpson, A. J.; Simpson,  
643 M. J. <sup>1</sup>H NMR-Based Metabolomics Investigation of *Daphnia Magna* Responses to Sub-Lethal  
644 Exposure to Arsenic, Copper and Lithium. *Chemosphere* **2013**, *93* (2), 331–337.  
645 <https://doi.org/10.1016/j.chemosphere.2013.04.085>.
- 646 (44) Cresswell, T.; Metian, M.; Golding, L. A.; Wood, M. D. Aquatic Live Animal Radiotracing Studies for  
647 Ecotoxicological Applications: Addressing Fundamental Methodological Deficiencies. *Journal of*  
648 *Environmental Radioactivity* **2017**, *178–179*, 453–460.  
649 <https://doi.org/10.1016/j.jenvrad.2017.05.017>.
- 650 (45) Magnusson, B. *The Fitness for Purpose of Analytical Methods: A Laboratory Guide to Method*  
651 *Validation and Related Topics (2nd Ed. 2014)*; Eurachem, 2014.
- 652 (46) Kragten, J. Tutorial Review. Calculating Standard Deviations and Confidence Intervals with a  
653 Universally Applicable Spreadsheet Technique. *Analyst* **1994**, *119* (10), 2161–2165.  
654 <https://doi.org/10.1039/AN9941902161>.
- 655 (47) Vigier, N.; Decarreau, A.; Millot, R.; Carignan, J.; Petit, S.; France-Lanord, C. Quantifying Li Isotope  
656 Fractionation during Smectite Formation and Implications for the Li Cycle. *Geochimica et*  
657 *Cosmochimica Acta* **2008**, *72* (3), 780–792. <https://doi.org/10.1016/j.gca.2007.11.011>.

- 658 (48) Bastian, L.; Vigier, N.; Reynaud, S.; Kerros, M.-E.; Revel, M.; Bayon, G. Lithium Isotope  
659 Composition of Marine Biogenic Carbonates and Related Reference Materials. *Geostandards and*  
660 *Geoanalytical Research* **2018**, *42* (3), 403–415. <https://doi.org/10.1111/ggr.12218>.
- 661 (49) R Core Team. R: A Language and Environment for Statistical Computing. *R Foundation for*  
662 *Statistical Computing, Vienna, Austria*. URL <https://www.R-project.org> **2017**.
- 663 (50) Millot, R.; Guerrot, C.; Vigier, N. Accurate and High-Precision Measurement of Lithium Isotopes in  
664 Two Reference Materials by MC-ICP-MS. *Geostandards and Geoanalytical Research* **2004**, *28* (1),  
665 153–159. <https://doi.org/10.1111/j.1751-908X.2004.tb01052.x>.
- 666 (51) Carignan, J.; Vigier, N.; Millot, R. Three Secondary Reference Materials for Lithium Isotope  
667 Measurements: Li7-N, Li6-N and LiCl-N Solutions. *Geostandards and Geoanalytical Research*  
668 **2007**, *31* (1), 7–12. <https://doi.org/10.1111/j.1751-908X.2007.00833.x>.
- 669 (52) Thibon, F.; Weppe, L.; Vigier, N.; Churlaud, C.; Lacoue-Labarthe, T.; Metian, M.; Cherel, Y.;  
670 Bustamante, P. Large Scale Survey of Lithium Concentrations in Marine Organisms. *Stoten* **under**  
671 **review**.
- 672 (53) Warnau, M.; Teyssié, J.-L.; Fowler, S. W. Cadmium Bioconcentration in the Echinoid *Paracentrotus*  
673 *Lividus*: Influence of the Cadmium Concentration in Seawater. *Marine Environmental Research*  
674 **1997**, *43* (4), 303–314. [https://doi.org/10.1016/S0141-1136\(96\)00093-1](https://doi.org/10.1016/S0141-1136(96)00093-1).
- 675 (54) Apeti, D. A.; Lauensteirn, G. G.; Johnson, E.; Kimbrough, K.; Mason, A. L. Mussel Watch Sampling  
676 Procedures and Site Descriptions for Oregon State. **2017**. <https://doi.org/10.25923/DAJ6-KK55>.
- 677 (55) Johnson, C. M.; Beard, B. L.; Albarède, F. *Geochemistry of Non-Traditional Stable Isotopes*; 2004;  
678 Vol. 55.
- 679 (56) Bouret, Y.; Poet, M.; Vigier, N.; Counillon, L.; Jarretou, G.; Bendahhou, S.; Montanes, M.; Thibon,  
680 F.; Balter, V. Biological Fractionations of Lithium Isotopes by Cellular Ion Exchangers Demonstrate  
681 Novel Modes of Transport. *submitted* **2021**.

- 682 (57) Counillon, L.; Bouret, Y.; Marchiq, I.; Pouyssegur, J. Na<sup>+</sup>/H<sup>+</sup> Antiporter (NHE1) and Lactate/H<sup>+</sup>  
683 Symporters (MCTs) in PH Homeostasis and Cancer Metabolism. *Biochimica et Biophysica Acta*  
684 *(BBA)-Molecular Cell Research* **2016**, *1863* (10), 2465–2480.  
685 <https://doi.org/10.1016/j.bbamcr.2016.02.018>.
- 686 (58) Grinstein, S.; Rotin, D.; Mason, M. J. Na<sup>+</sup>/H<sup>+</sup> Exchange and Growth Factor-Induced Cytosolic PH  
687 Changes. Role in Cellular Proliferation. *Biochimica et Biophysica Acta (BBA)-Reviews on*  
688 *Biomembranes* **1989**, *988* (1), 73–97. [https://doi.org/10.1016/0304-4157\(89\)90004-X](https://doi.org/10.1016/0304-4157(89)90004-X).
- 689 (59) Milosavljevic, N.; Monet, M.; Léna, I.; Brau, F.; Lacas-Gervais, S.; Feliciangeli, S.; Counillon, L.;  
690 Poët, M. The Intracellular Na<sup>+</sup>/H<sup>+</sup> Exchanger NHE7 Effects a Na<sup>+</sup>-Coupled, but Not K<sup>+</sup>-Coupled  
691 Proton-Loading Mechanism in Endocytosis. *Cell reports* **2014**, *7* (3), 689–696.  
692 <https://doi.org/10.1016/j.celrep.2014.03.054>.
- 693 (60) Jakobsson, E.; Argüello-Miranda, O.; Chiu, S.-W.; Fazal, Z.; Kruczek, J.; Nunez-Corrales, S.; Pandit,  
694 S.; Pritchett, L. Towards a Unified Understanding of Lithium Action in Basic Biology and Its  
695 Significance for Applied Biology. *J Membr Biol* **2017**, *250* (6), 587–604.  
696 <https://doi.org/10.1007/s00232-017-9998-2>.
- 697 (61) Herchuelz, A.; Van Eylen, F.; Lebrun, P. L'échange Na/Ca. *médecine/science* **1995**, *11*, 232–238.
- 698 (62) Palty, R.; Ohana, E.; Hershfinkel, M.; Volokita, M.; Elgazar, V.; Beharier, O.; Silverman, W. F.;  
699 Argaman, M.; Sekler, I. Lithium-Calcium Exchange Is Mediated by a Distinct Potassium-  
700 Independent Sodium-Calcium Exchanger. *Journal of Biological Chemistry* **2004**, *279* (24), 25234–  
701 25240. <https://doi.org/10.1074/jbc.M401229200>.
- 702 (63) Rollion-Bard, C.; Blamart, D. Possible Controls on Li, Na, and Mg Incorporation into Aragonite  
703 Coral Skeletons. *Chemical Geology* **2015**, *396*, 98–111.  
704 <https://doi.org/10.1016/j.chemgeo.2014.12.011>.

- 705 (64) Rollion-Bard, C.; Vigier, N.; Meibom, A.; Blamart, D.; Reynaud, S.; Rodolfo-Metalpa, R.; Martin, S.;  
706 Gattuso, J.-P. Effect of Environmental Conditions and Skeletal Ultrastructure on the Li Isotopic  
707 Composition of Scleractinian Corals. *Earth and Planetary Science Letters* **2009**, *286* (1–2), 63–70.  
708 <https://doi.org/10.1016/j.epsl.2009.06.015>.
- 709 (65) Freitas, P. S.; Clarke, L.; Kennedy, H.; Richardson, C. Inter- and Intra-Specimen Variability Masks  
710 Reliable Temperature Control on Shell Mg/Ca Ratios in Laboratory- and Field-Cultured *Mytilus*  
711 *Edulis* and *Pecten Maximus* (Bivalvia). **2008**. <https://doi.org/10.5194/BG-5-1245-2008>.
- 712 (66) Marriott, C. S.; Henderson, G. M.; Belshaw, N. S.; Tudhope, A. W. Temperature Dependence of  
713  $\Delta 7\text{Li}$ ,  $\Delta 44\text{Ca}$  and Li/Ca during Growth of Calcium Carbonate. *Earth and Planetary Science Letters*  
714 **2004**, *222* (2).
- 715 (67) Stokes, P. E.; Okamoto, M.; Lieberman, K. W.; Alexander, G.; Triana, E. Stable Isotopes of Lithium:  
716 In Vivo Differential Distribution between Plasma and Cerebrospinal Fluid. *Biol. Psychiatry* **1982**,  
717 *17* (4), 413–421.
- 718 (68) Figueroa, L. T.; Razmillic, B.; Zumeata, O.; Aranda, G. N.; Barton, S. A.; Schull, W. J.; Young, A. H.;  
719 Kamiya, Y. M.; Hoskins, J. A.; Ilgren, E. B. Environmental Lithium Exposure in the North of Chile--II.  
720 Natural Food Sources. *Biol Trace Elem Res* **2013**, *151* (1), 122–131.  
721 <https://doi.org/10.1007/s12011-012-9543-1>.
- 722 (69) Roux, M.; Dosseto, A. From Direct to Indirect Lithium Targets: A Comprehensive Review of Omics  
723 Data. *Metallomics* **2017**, *9* (10), 1326–1351. <https://doi.org/10.1039/C7MT00203C>.
- 724 (70) Figueroa, L. T.; Barton, S. A.; Schull, W. J.; Young, A. H.; Kamiya, Y. M.; Hoskins, J. A.; Ilgren, E. B.  
725 Environmental Lithium Exposure in the North of Chile - Tissue Exposure Indices. *Epidemiology,*  
726 *Biostatistics and Public Health* **2014**, *11* (1). <https://doi.org/10.2427/8847>.

- 727 (71) Viana, T.; Ferreira, N.; Henriques, B.; Leite, C.; De Marchi, L.; Amaral, J.; Freitas, R.; Pereira, E.  
728 How Safe Are the New Green Energy Resources for Marine Wildlife? The Case of Lithium.  
729 *Environmental Pollution* **2020**, *267*, 115458. <https://doi.org/10.1016/j.envpol.2020.115458>.
- 730 (72) Verney-Carron, A.; Vigier, N.; Millot, R.; Hardarson, B. S. Lithium Isotopes in Hydrothermally  
731 Altered Basalts from Hengill (SW Iceland). *Earth and Planetary Science Letters* **2015**, *411*, 62–71.  
732 <https://doi.org/10.1016/j.epsl.2014.11.047>.
- 733 (73) Broecker, W. S.; Peng, T.-H. *Tracers in the Sea*; Eldigio Press: Palisades, N.Y., 1982.
- 734 (74) Huh, Y.; Chan, L.-H.; Zhang, L.; Edmond, J. M. Lithium and Its Isotopes in Major World Rivers:  
735 Implications for Weathering and the Oceanic Budget. *Geochimica et Cosmochimica Acta* **1998**, *62*,  
736 2039–2051. [https://doi.org/10.1016/S0016-7037\(98\)00126-4](https://doi.org/10.1016/S0016-7037(98)00126-4).
- 737 (75) Seidel, U.; Baumhof, E.; Hägele, F. A.; Bosy-Westphal, A.; Birringer, M.; Rimbach, G. Lithium-Rich  
738 Mineral Water Is a Highly Bioavailable Lithium Source for Human Consumption. *Molecular*  
739 *Nutrition & Food Research* **2019**, *63* (13), 1900039. <https://doi.org/10.1002/mnfr.201900039>.
- 740 (76) Young, W. Review of Lithium Effects on Brain and Blood. *Cell Transplant* **2009**, *18* (9), 951–975.  
741 <https://doi.org/10.3727/096368909X471251>.
- 742 (77) Nunes, M. A.; Buck, T. A. V. and H. S. Microdose Lithium Treatment Stabilized Cognitive  
743 Impairment in Patients with Alzheimer’s Disease <https://www.eurekaselect.com/106398/article>  
744 (accessed Oct 19, 2020).
- 745